Flexibility of "Polyunsaturated Fatty Acid Chains" and Peptide Backbones: A Comparative ab Initio Study

Jacqueline M. S. Law,[†,‡] David H. Setiadi,[†,‡] Gregory A. Chass,[§] Imre G. Csizmadia,[†,‡] and Béla Viskolcz*[,‡]

Department of Chemistry, University of Toronto, Toronto, Ontario, Canada M5S 3H6; Department of Chemistry and Chemical Informatics, Faculty of Education, University of Szeged, Szeged, Boldogasszony sgt. 6, Hungary 6725; and Institute of Biocomputations and Physics of Complex Systems, Department of Theoretical Physics, University of Zaragoza, Zaragoza, Spain 50009

Received: August 12, 2004

The conformational properties of ω-3 type of polyunsaturated fatty acid (PUFA) chains and their fragments were studied using Hartree−Fock (RHF/3-21G) and DFT (B3LYP/6-31G(d)) methods. Comparisons between a unit (**U**) fragment of the PUFA chain and a mono *N*-Ac-glycine-NHMe residue show that both structures have the same sequence of $sp^2-sp^3-sp^2$ atoms. The flexibility of PUFA originates in the internal rotation about the above pairs of σ bonds. Therefore, potential energy surfaces (PESs) were generated by a scan around the terminal dihedral angles (ϕ_{t1} and ϕ_{t2}) as well as the ϕ_1 and ψ_1 dihedrals of both **1U** congeners (Me−CHCH−CH_2−CHCHMe and MeCONH−CH_2−CONHMe) at the RHF/3-21G level of theory. An interesting similarity was found in the flexibility between the cis allylic structure and the trans peptide models. A flat landscape can be seen in the cis **1U** (hepta-2,5-diene) surface, implying that several conformations are expected to be found in this (PES). An exhaustive search carried out on the **1U** and **2U** models revealed that straight chain structures such as trans and cis beta ($\phi_1 \approx \psi_1 \approx 120°$; $\phi_2 \approx \psi_2 \approx -120°$) or trans and cis extended ($\phi_1 \approx \psi_1 \approx \phi_2 \approx \psi_2 \approx 120°$) can be formed at the lowest energy of both isomers. However, forming helical structures, such as trans helix ($\phi_1 \approx -120°$, $\psi_1 \approx 12°$; $\phi_2 \approx -120°$, $\psi_2 \approx 12°$) or cis helix ($\phi_1 \approx -130°$, $\psi_1 \approx 90°$; $\phi_2 \approx -145°$, $\psi_2 \approx 90°$) will require more energy. These six conformations, found in **2U**, were selected to construct longer chains such as **3U**, **4U**, **5U**, and **6U** to obtain the thermochemistry of secondary structures. The variation in the extension or compression of the chain length turned out to be a factor of 2 between the helical and nonhelical structures. The inside diameter of the "tube" of cis helix turned out to be 3.5 Å after discounting the internal H atoms. Thermodynamic functions were computed at the B3LYP/6-311+G(2d,p)//B3LYP/6-31G(d). The cis−trans isomerization energy of 1.7 ± 0.2 kcal mol^{-1} $unit^{-1}$ for all structure pairs indicates that the conformer selection was consistent. A folding energy of 0.5 ± 0.1 kcal mol^{-1} $unit^{-1}$ has been extracted from the energy comparison of the helices and most extended nonhelical structures. The entropy change associated with the folding ($\Delta S_{folding}$) is decreases faster with the degree of polymerization (n) for the cis than for the trans isomer. As a consequence, the linear relationships between ($\Delta G_{folding}$) and n for the cis and trans isomer crossed at about $n = 3$. This suggested that the naturally occurring cis isomer less ready to fold than the trans isomer since a greater degree of organization is exhibited by the cis isomer during the folding process. The result of this work leads to the question within the group additivity rule: could the method applied in our study of the folding of polyallylic hydrocarbons be useful in investigating the thermochemistry of protein folding?

Introduction

Polymers containing π bonds (Figure 1) and a repeating sequence of $sp^2-sp^3-sp^2$ atoms are naturally observed in polyunsaturated fatty acids (PUFA) as the cis isomer[1] and in peptide backbone as a trans isomers. These two congeneric molecular structures differ only by a few atoms (Figure 2). Both structures contain CH_2 groups placed between two σ bonds that can rotate to different conformations with the investment of a small amount of energy.[2] Despite the low energy barrier, the backbone of polypeptides is still very rigid as a result of the formation of stabilizing intramolecular H-bonds.[3] However, such intramolecular forces are missing in PUFA chains. Consequently, the low energy barrier, in addition to the high degree

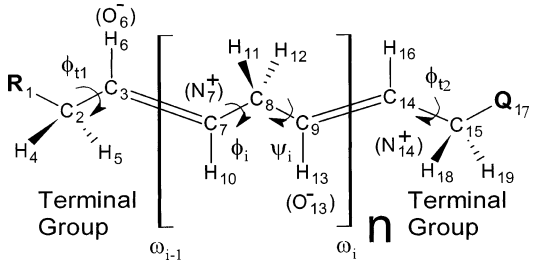

Figure 1. A general polyallylic structure with definition and numbering of all atoms for allyl and peptide (heteroatoms in parentheses) models (where Q = P = CH_3 and $0 \le n \ge 6$ in the present study). For ω-3 and ω-6 PUFAs Q is $-CH_2-COOH$, R group is CH_3 or $CH_3-(CH_2)_3-$, respectively.

† University of Toronto.
‡ University of Szeged.
§ University of Zaragoza.
* Corresponding author: e-mail viskolcz@jgytf.u-szeged.hu.

10.1021/jp040546y CCC: $30.25
Published on Web 12/30/2004

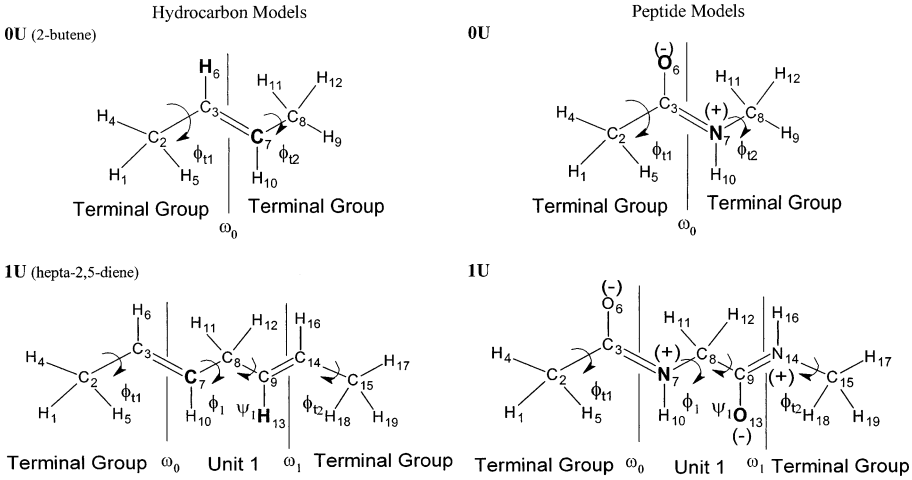

Figure 2. Comparison between polyallylic and polyglycine systems in terms of **0U** and **1U** hydrocarbon and peptide models The peptide structures are shown in their zwitterionic resonance structures to call attention to their structural similarities to the hydrocarbon models.

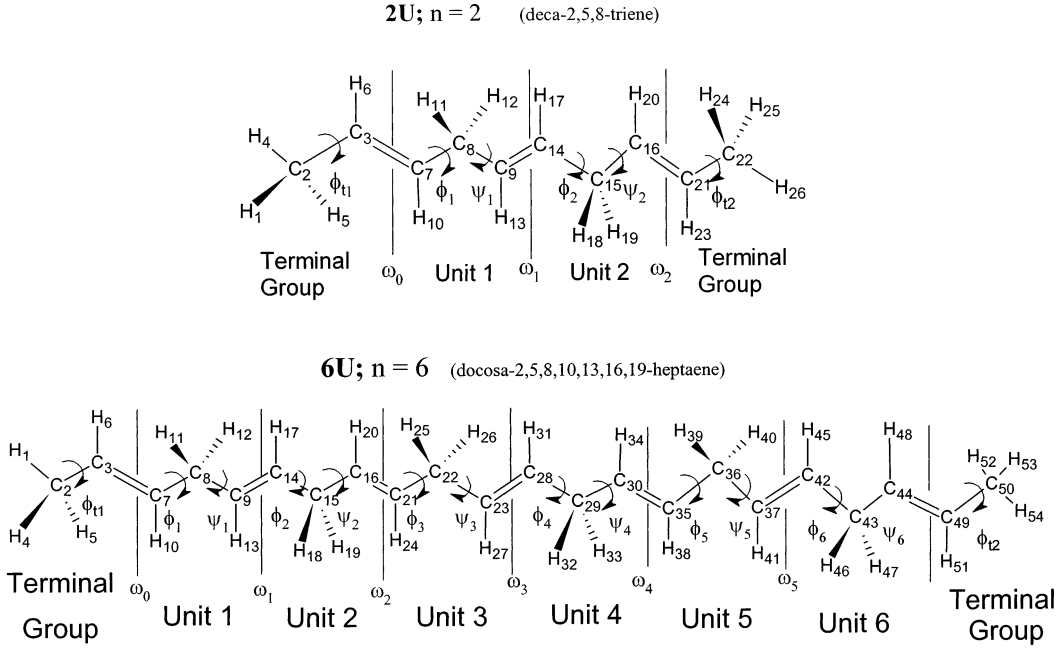

Figure 3. Structures of **2U** and **6U** models.

of unsaturation, results in an increase in flexibility,[2] and many studies have been carried out to investigate such properties in relation to the structure and function of the lipid bilayer.[2] These general relationships will be summarized in the next section. The similarities and differences of the two types of polymers can help us to better understand the folding processes and membrane flexibility.

Characterization of PUFAs. When incorporated into the bilayer, the flexibility of PUFA may lead to certain modifications to the microenvironment, including a loss of rigidity, increase in water permeability,[4] decrease of phase transition temperature,[5] and, as a whole, change in packing volume.[6] The abundance of π-bonds found in ω-3 fatty acid chains also makes the bilayer more vulnerable to free radical attack;[7,8] therefore, it is part of the defense mechanism. Neurons, which contain a high amount of polyunsaturated fatty acid, are especially sensitive to lipid peroxidation. Alzheimer's disease (AD) is believed to related to such free radical reactions with membrane lipids in the brain.[9]

Earlier MMX computations[10] have shown that an allylic chain can fold into two main structures. The first, called "extended", occurs when all the π-bonds form planes, analogous to the amide planes in peptides, and each is rotated 90° with respect to the adjacent plane. The other structure found is the "iron angle",[10] where the adjacent planes are rotated in alternating +90° and −90°.[11−15] These two structures are proposed to exist normally in a lipid bilayer with a relatively low packing energy.[10] However, other studies have found a third structure, similar to a peptide helix,[16] which exists in arachidonic acid-abundant lipid bilayers. Therefore, unsaturated chains of various lengths (Figure 3) were investigated to obtain the conformational properties and the cis−trans isomerization enthalpy as well as the folding processes of long flexible polyunsaturated but nonconjugated hydrocarbons.

Figure 1 shows the general monomer of the polyallylic and peptide chains under investigation, where n is the number of units or "degree of polymerization" (i.e., $0 \leq n \leq 6$). Studying the secondary structures of these allylic chains can lead to a better understanding of the role of all PUFAs play in determining membrane properties. Specifically, the folding of PUFA chains into various secondary structures may create different structural environments in the lipid bilayer that will undoubtedly correspond to different levels of susceptibility toward lipid per-

oxidation initiated by superoxide anion (O_2^-) or other highly reactive oxygen species (ROS).[17]

Folding of Allylic Groups. Up until now, no experimental evidence has been found to describe each specific conformational structure of polyallylic chains. Recent NMR studies of polyunsaturated phospholipids have shown that PUFAs are flexible and are able to form large number conformations.[18] It was also suggested that acyl chains contain three or more double bonds; each of the individual σ bonds could not rotate as freely into different conformations and is actually highly ordered and therefore not as "fluid" as was generally believed.[19] X-ray crystallography studies have shown that PUFAs can also interact with various proteins by folding into structures similar to peptide secondary structures.[20,21] This implies that without hydrogen bonding and side-chain interactions the folding properties governing peptide and hydrocarbon backbones may be similar.

Structural Analogy between Polypeptides and Polyallylic Systems. Polypeptides are known to fold into α-helix,[22] β-sheet,[22] and β-hairpin[23] secondary structures stabilized by intramolecular hydrogen bonds. In addition to the above secondary structures of the polypeptide backbone, side chains may interact with each other to promote further peptide folding. For example, additional interactions between the aromatic side chain and hydrogen atom of the amine group[24] as well as those between cis proline and aromatic side chains[25] can affect peptide folding. To predict and quantify the effects of such interactions may exert on the folding the proteins, intense computations have been performed on short peptide fragments containing various combinations of side chains.[26−30] As shown in Figure 2, polyallylic systems are structurally analogous to the polyglycine system because both backbones contain atoms with repeating $sp^2-sp^3-sp^2$ hybridized states. From previous studies, it was shown that helical and strandlike secondary structures similar to those in peptides can also exist in the polyallylic system.[10]

In the next section, we will describe a strategy to obtain the same conformations in chain models with different degrees of polymerization. Then, the geometric properties of the most extended and the least extended structure will be compared. In the final part, the secondary structures the trans allylic system will be compared to those of the peptides.

Method

Strategy of Conformational Study. Seven allylic models were selected to investigate the general allylic system (Figure 1), and each of their degrees of freedom was defined in a manner similar to the peptide definition previously developed.[29,30] First, the allylic fragments were separated into identical units (**U**) with [=CH−CH_2−CH=] monomers. Then terminal Me−CH= and =CH−Me groups were added to these fragments to complete the model. Such groups were chosen because their structures are simple and will not increase steric hindrance. Furthermore, this procedure is similar to the addition of protecting methyl groups in the *N*-Ac-$(Gly)_n$-NHMe models.

Model **0U** (2-butene) was the first molecule to be studied. It is different from the rest of the models because it contains only one π-bond; that is, only the two terminal groups are joined together. It does not have any CH_2 groups that separate the two adjacent double bonds and is therefore lacking the general allylic patterns shown in Figure 2. A single scan was carried out on the terminal dihedrals ϕ_{t1} and ϕ_{t2} of **0U** ($n = 0$) at the RHF/3-21G level of theory followed by optimization of the cis and trans isomer of **0U** at the same level. In addition, a single scan was also performed on the 0th model of a peptide bond, MeCO−NHMe, that contains the protective groups at the two termini.

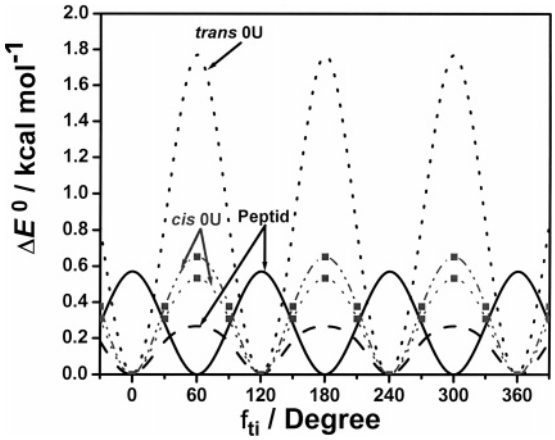

Figure 4. Potential energy curves for scans of the **0U** allylic and peptide models. The two curves for the cis **0U** are associated with staggered and eclipsed orientations of the nonrotating methyl group.

The smallest possible fragment, **1U** ($n = 1$; C_7H_{12}), contains all the components (one complete unit and two methyl terminal groups) of the general polyallylic models in this study. The potential energy surfaces for the cis and trans isomers of **1U** were obtained by performing a double scan around ϕ_1 and ψ_1 at the RHF/3-21G level of theory. Complementary optimizations on all possible conformations of **1U** were also carried out at the same level of theory. In addition, a double scan for *N*-Ac-Gly-NHMe was also computed to compare with that of the **1U** model at the RHF/3-21G level of theory.

In **2U** ($n = 2$; $C_{10}H_{16}$), all predicted conformations were computed at the RHF/3-21G level of theory. In total, 81 conformations were predicted for each isomer, and for each isomer all the π bonds were found only in either the cis or trans configuration. The definition of cis and trans isomers was also applied to the larger models. It should be noted that, with the addition of each unit, the number of possible conformations for a given isomer increases by a factor of 9. With this exponential increase in parameters, such an approach of conformational study would quickly become impractical. Thus, exhaustive conformational searches were not carried out beyond **2U**. Instead, specific conformations of **2U** were applied, by consecutive repetitions, to construct **3U**, **4U**, **5U**, and **6U** oligomers (Figure 3) corresponding to $C_{13}H_{20}$, $C_{16}H_{24}$, $C_{19}H_{28}$, and $C_{23}H_{32}$, respectively. Six conformations (trans beta, trans extended, trans helix, cis beta, cis extended, cis helix) were selected to construct larger models of **3U**, **4U**, **5U**, and **6U**, which were optimized at the RHF/3-21G and B3LYP/6-31G(d) levels of theory.

Computational Methods. Every conformation was first optimized at the RHF/3-21G level of theory. To obtain more accurate relative energies, the selected conformers were reoptimized, and the harmonic frequencies were calculated at the B3LYP/6-31G(d) level of theory. Often, in the case of higher units, optimized RHF/3-21G results cannot produce a satisfactory guess for consecutive DFT optimization because the DFT optimization of shallow minima often leads to the discovery of new minima that are different from the one conformer found at the RHF/3-21G level of theory. The ZPE's were scaled using the factors of 0.89 and 0.96 for RHF/3-21G and for B3LYP/6-31G(d), respectively.[31] Each calculation was conducted using the Gaussian98 or Gaussian03 program packages.[32,33]

Results and Discussion

Conformations of End Groups. Single scans were carried out on the smallest structures **0U** of the two congeners followed

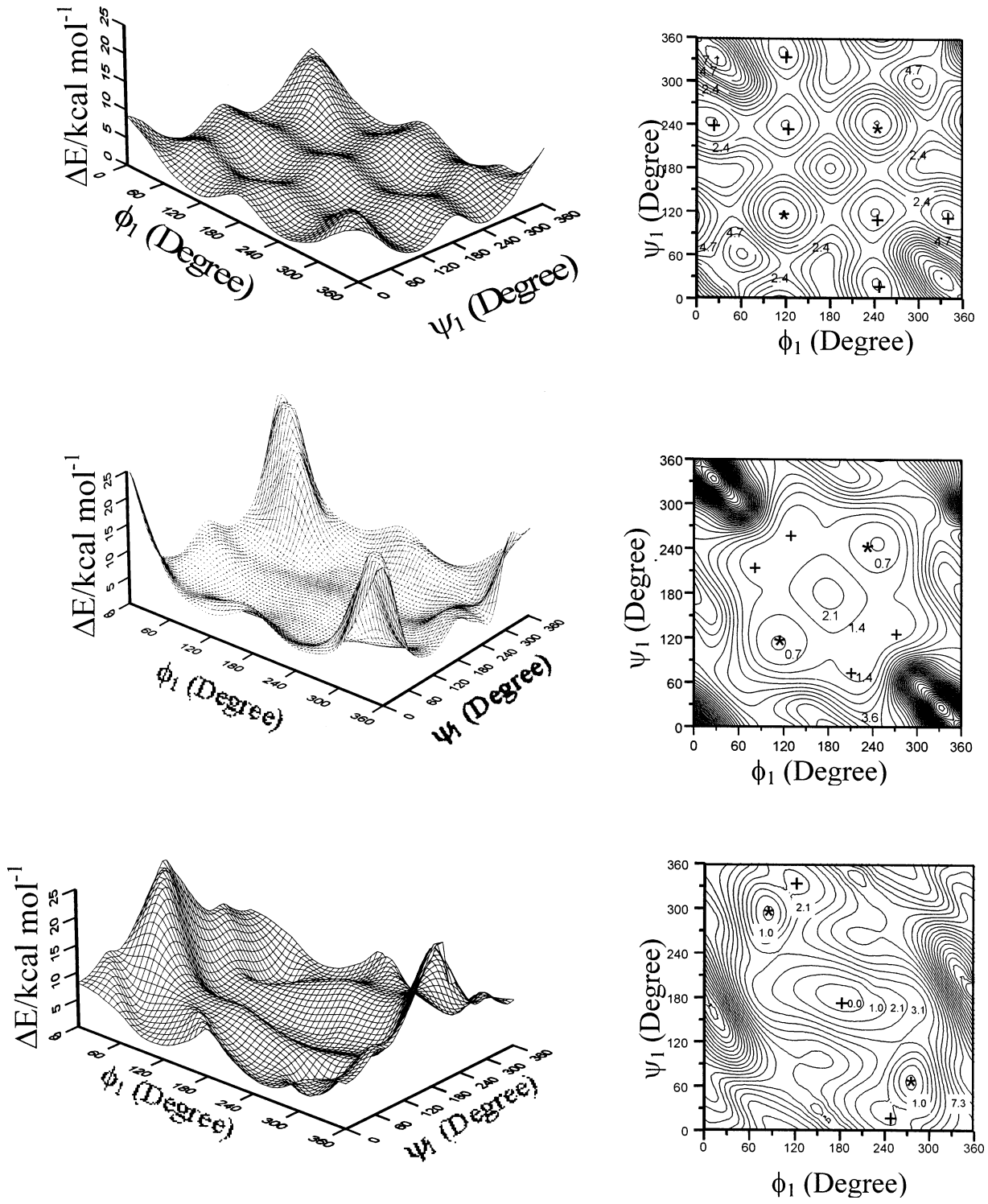

Figure 5. Conformational PES's for trans **1U**, cis **1U**, and the two different function of the cis **0U** are associated with trans−trans Ac-*N*-Gly-NHMe, from top to bottom, respectively. The global and local minima are marked by * and +, respectively.

by an exhaustive conformational search at the RHF/3-21G level of theory to find all possible minima. A comparison between the scans of **0U** and the peptide bond revealed that ϕ_{t1} minima are located in positions different from those in peptides. As shown in Figure 4, the ϕ_{t1} of the trans and cis **0U** hydrocarbon are shifted to the eclipse position; ϕ_{t1} of the peptide remained in the stagger position. However, the minima for ϕ_{t2} of both molecules are found at 0°, 120°, and −120°. This implies that the dihedrals at the carboxyl end of peptides are similar to that of an allylic methyl dihedral.

Scans and Optimizations of 1U. Model **1U** contains one allylic group and two terminal groups. The π-bonds of the sp^2 carbons are defined at ω_i while the σ-bonds of the sp^3 carbon are defined as ϕ_i and ψ_I (Figure 3) A double relaxed scan was carried out at the RHF/3-21G level of theory to assess the potential energy surface as a function of ϕ and ψ. As can be seen in Figure 5, the global minima for trans **1U** and cis **1U** have ϕ and ψ values near 120°. The trans surface (Figure 5, top) reveals that all minima and barriers of ϕ and ψ are found in similar locations as those in Figure 4, with barrier heights of

TABLE 1. Energy (hartrees), Energies Relative to Trans (+ +/− −) in kcal mol^{-1}, and Dihedral Values of 1U for All Possible Trans (Top) and Cis (Bottom) Isomers at the RHF/3-21G Level of Theory

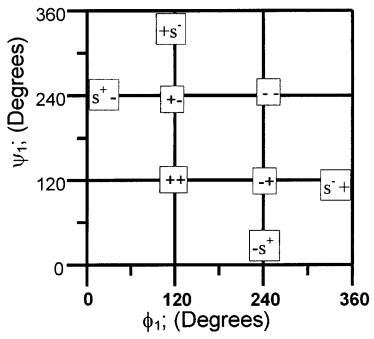

Trans

Conformation	ϕ_{t1}	ϕ_1	ψ_1	ϕ_{t2}	ΔE_{Rel} (kcal*mol)
-(--)+	-120.783	-116.767	-117.357	120.121	0.0
-(++)+	-120.294	117.149	117.150	120.590	0.0
+(*s*$^+$-)+	120.571	16.729	-115.704	119.972	0.8
+(*s*$^-$+)+	120.506	-16.738	115.697	120.905	0.8
+(+*s*$^-$)+	121.014	115.559	-16.888	120.432	0.8
-(-*s*$^+$)+	-120.883	-115.645	16.600	120.717	0.8
+(+-)+	120.592	118.980	-119.067	120.328	0.9
+(-+)+	120.541	-119.009	118.960	120.452	0.9

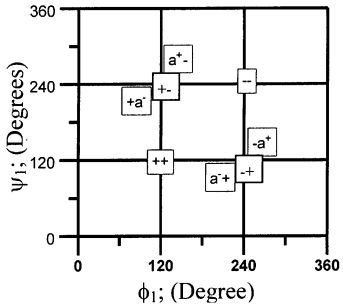

Cis[a]

+(--)+	121.4125	-114.720	-115.163	121.560	3.6
+(++)+	120.6472	115.229	115.096	120.534	3.6
+(+-)+	119.9434	119.604	-119.733	121.796	4.3
+(-+)+	121.8812	-119.701	119.759	119.842	4.3

[a] +a$^-$;a$^+$−; a$^-$+;− a$^+$ conformers of cis **1U** are very hard to optimize, and they appear to coalesce to the remaining four minima listed in the cis part of the table.

approximately 2 kcal mol^{-1}. The flexibility difference between the rotation about σ C−C bonds of the $-CH_2-$ in the trans units and the terminal $-CH_3$ group is negligible. On the other hand, the cis **1U** PES (middle in Figure 5) reveals a rather different picture. A very flat hexagonal area dominates the central part of the PES that has a 45° inclination from the horizontal axis (ϕ axis). As a result, the rotation barriers are very small between minima that are very shallow themselves. The barriers at the edges of the surface are significantly higher. This implies that the cis isomer can form several different conformers relatively easily. Any slight steric effect or H repulsions between remote allylic groups will have a very large influence on the minima that would be found in the cis isomer. In our next paper, we will discuss this in detail.[34] Although a smooth basin was observed in the scans, only one pair conformation of **1U** was found to have dihedral values at +120° or −120°. The pair of stable conformations resulted from the coalescence tree pair of conformers are included in Table 1. An additional double scan of trans *N*-Ac-Gly-NHMe was also carried out at the RHF/3-21G level of theory (Figure 5, bottom), and it was compared to that of the **1U** surface, which revealed that there are some similarities between the "trans peptide" surface and that of cis **1U**. For example, there are also flat areas along the line of $\psi = -\phi$. However, unlike the cis **1U** PES, there are addition barriers that are probably the result of stabilizing intramolecular hydrogen bonding.

Conformational Study of 2U. In the next step, the **1U** model was extended to **2U** ($n = 2$, $C_{10}H_{16}$). To characterize all possible cis and trans minima here, an exhaustive search was carried out at the RHF/3-21G level of theory. To compare the conformers of **2U** with **1U**, all ψ values of **2U** conformations found were plotted against their ϕ values (Figure 6, top). The distribution of these points shows that all the conformers found are located in areas corresponding to the minima shown in Figure 5. The trans **2U** conformations are concentrated in the minima of the trans **1U** PES, while the cis **2U** points were more loosely distributed in the flat basin as seen in the cis **1U** PES. The bottom of Figure 6 shows all stable conformers from every model at both levels of theory collected from the present study to illustrate the consistency of calculations, and these results will be discussed in later sections. The conformers selected to build longer chains are listed in Table 2. (All conformers found and their relative electronic energies are listed in Table 1 of the Supporting Information.) We should note that the exhaustive search that was made included symmetrical molecules, while in the case of the fatty acids, the loss of symmetry was caused

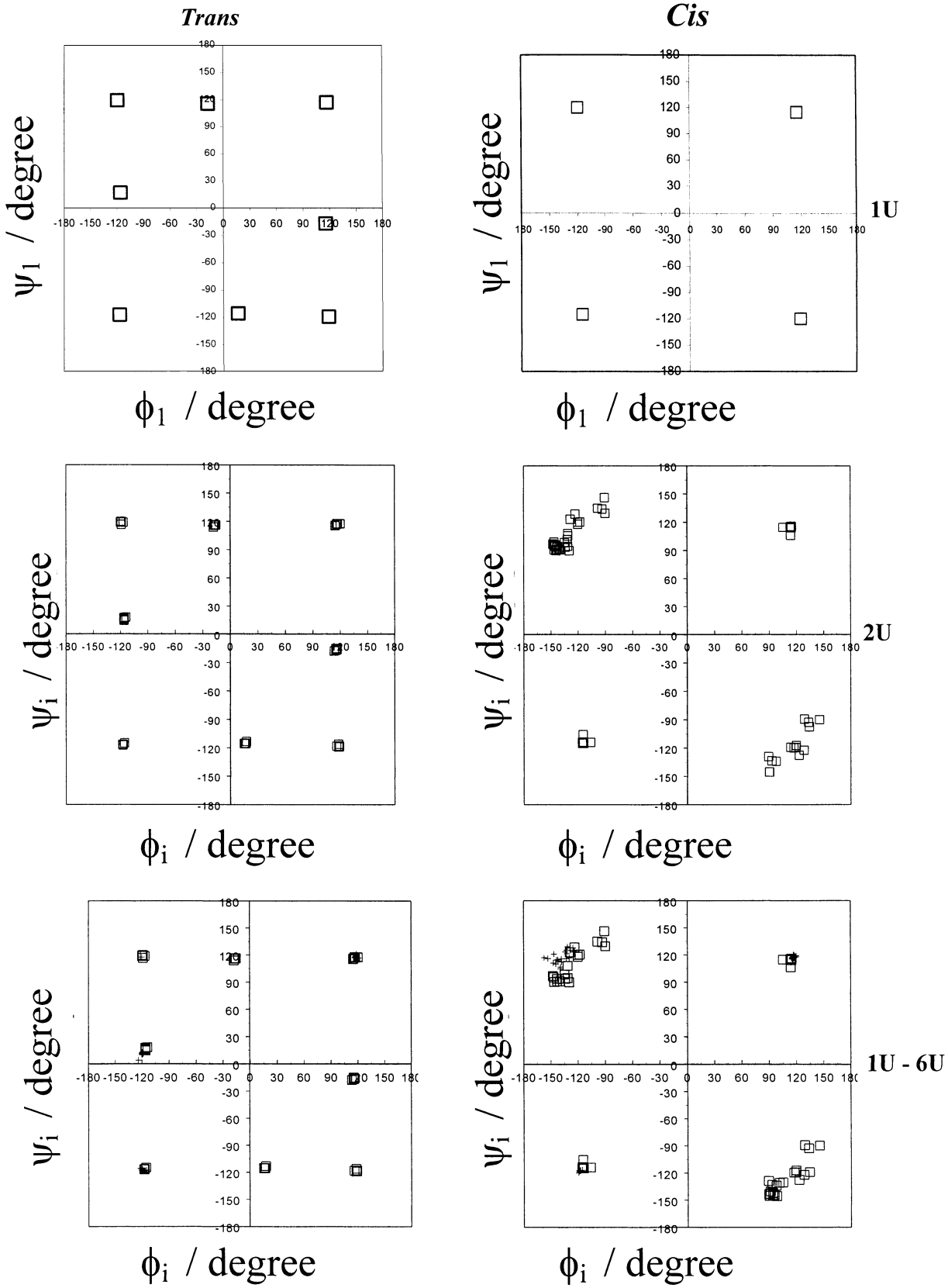

Figure 6. ϕ_i and ψ_i distribution in all-trans (left side) and in all-cis isomers (right side). The top and middle rows of charts show **1U** and **2U** optimizations, respectively. The bottom row shows all the optimized minima of **1U**−**6U** combined. The (□) and (+) represent dihedral values obtained by RHF/3-21G(d) and by B3LYP/6-31G(d) optimization, respectively.

by the difference in terminal groups **Q** and **R** (see Figure 1). Consequently, a number of the conformers listed are identical structures within the accuracy of optimization. This observation implies that such allylic dihedral patterns are consistent regardless of the degree of polymerization. However, some **2U** optimizations led to new stable conformations involving a^+ or a^- orientations, which were difficult to optimize in the case of **1U**. Polymerization results in the increase of the number of

TABLE 2. Dihedral Values and Relative Energies of 2U Conformers Were Selected To Construct Longer Chains Obtained at the RHF/3-21G Level of Theory[a]

	conformations[b]	ϕ_{t1}	ϕ_1	ψ_1	ϕ_2	ψ_2	ϕ_{t2}	ΔE[c]
trans	+(+ + − −)+	120.599	117.031	116.916	−117.030	−116.969	120.301	0.0
	−(+ + + +)+	−120.380	117.062	116.735	116.772	116.705	120.472	0.0
	+(−s$^+$−s$^+$)+	120.147	−115.614	15.305	−115.885	15.930	120.467	1.6
cis	+(+ + + +)+	120.625	114.776	114.873	114.892	114.825	120.636	5.5
	+(+ + − −)+	−121.246	114.968	115.189	−115.154	−114.978	121.275	5.6
	+(a$^-$+a$^-$+)+	123.840	−133.642	93.249	−145.747	90.118	113.610	6.7

[a] All possible conformers are listed in Table 1 of the Supporting Information. [b] Extended conformations = (+ + + +); beta conformation = (+ + − −); helical conformation = (−s$^+$−s$^+$) or (a$^-$+a$^-$+). [c] Relative energy to trans (+ + + +) conformation in kcal mol^{-1}.

stable conformations and also adds stability to various possible secondary structures. One explanation for this may be that such conformers allow not only for interactions between nearest neighboring allylic groups but also with the remote ones, leading to the formation of a "smooth basin" and an increase in the number of conformations observed in **2U**.

It is interesting to note that in **2U** there are 81 possible conformations for each of the isomers, but only 65 and 21 were found for the trans and cis form, respectively. However, the formation of these geometries is not random. For the trans isomer, however, the conformations found in a given unit is independent of the neighboring units. In fact, it is observed that within one unit a dihedral with syn$^-$ or syn$^+$ (s$^-$ or s$^+$) values must pair with dihedrals that are in the conformation of + or −, respectively. Therefore, $\phi_I = -120°$ and $\psi_I = +12°$ must be regarded to be equivalent to $\phi_I = 120°$ and $\psi_I = -12°$, and vice versa. In cis **2U** there are even more restrictions on allowed conformations. For example, + and − cannot exist in the same unit, and anti$^+$ (a$^+$) must pair with −. In addition, there seems to be some interdependency between the conformations of two adjacent units.

We have attempted to find the cis and trans global minima as well as various structures resembling helices and straight chains found in a beta strand. Six of such structures were found, and they were further optimized at the B3LYP/6-31G(d) level of theory. They were designated as trans beta (+ + − −) as the global minima, trans extended (+ + + +), trans helix (−s$^+$−s$^+$) one of the most compact structure, cis extended (+ + + +), cis beta (+ + − −), and cis helix (a$^-$+a$^-$+). For a definition of symbols specifying conformations see Table 1.

Selection of 2U Conformers for Building Larger Models. Table 2 also presents the ZPE corrected relative energies for selected conformations of **2U**. As can be seen in Table 3, the relative energies predict by RHF/3-21G and DFT are in fair agreement with each other within a 1 kcal mol^{-1} range. Both cis and trans conformers have two "quasi-global" minima energy conformers, indicated by (+ + + +) and (+ + − −). The energy differences between (+ + + +) and (+ + − −) conformers are smaller than 0.1 kcal mol^{-1}. Consequently, both minima were selected to build the larger models. The energy calculations of the larger fragments show that this difference remains negligibly small. Both cis and trans isomers also have the possible combination with (+ + + −) conformer. Its energy is in between the most (+ + + +) and the least (a$^-$+a$^-$+) extended structure. Therefore, this particular structure will not be included in the construction of larger models. Consequently, our interest was focused on the conformations with the lowest energy and/or structures that form peptide-like secondary structures with simple and conformationally equivalent units. The third possible periodic repeating conformers would be $\phi_i = \phi_{i+1} \approx -120°$ and $\psi_i = \psi_{i+1} \approx 12°$, which is the most favored (−s$^+$−s$^+$) trans helix conformers (Table 1). Therefore, it was also selected to build the larger chains. It should be emphasized that in the cis isomer the "smooth basin" of Figure 5 (middle) implies that multiple conformations may exist. This prediction was shown in the case of **2U** where a number of (a$^-$+a$^-$+) conformers were having an energy variation of less than 0.4 kcal mol^{-1}. Such flexibility can also explain some of the numerous unexpected problems in optimization of the selected conformers. However, this structure was also selected because it can form a helix.

Construction and Optimization of Higher Structures. The above six structures were selected from the cis and trans **2U** RHF/3-21G optimizations as basic building blocks for the construction of models **3U**, **4U**, **5U**, and **6U**. In all higher models, methyl groups were used (R = Q = CH_3) in terminal units (see Figure 1). These new structures were first optimized at the RHF/3-21G to obtain an initial geometry estimates, which were further optimized at the B3LYP/6-31G(d) level of theory. This procedure was repeated to build **3U**, **4U**, **5U**, and **6U**. Comparisons between the selected conformation of **2U** at RHF/3-21G (Table 2 and supplementary Table 1 highlighted by bold) and B3LYP/6-31G(d) (Table 3) show that, for most of the selected structures, the conformational differences between these two methods are less than 4°. They also show good agreement with the earlier MM calculation.[10] However, in the cis helices, the dihedrals obtained at two levels of theory differ from each other by 10°, 35°, 17°, and 32° for **3U**, **4U**, **5U**, and **6U**, respectively. Furthermore, the new geometries optimized by HF and DFT for the cis helix structures are significantly different from those predicted earlier by Applegate and Glomset.[10] This is understandable because ab initio HF, and especially DFT, take into account of the various long-range interactions and lead to the calculation of a significantly larger ensemble of the more compact cis conformers.

General Features of Larger Models. By increasing the chain length of **2U** by one unit while keeping the terminal groups with the ending CH_3, a larger model, **3U**, is obtained. The dihedral values of all models (**0U**−**6U**) obtained at B3LYP/6-31G(d) are collected in Table 2 of the Supporting Information. The relative energies and enthalpies at the RHF/3-21G, B3LYP/6-31G(d) and B3LYP/6-311+G(2d,p)//B3LYP/6-31G(d) levels of theory are listed in Table 3. Assessment of the **3U**, **4U**, **5U**, and **6U** geometries shows that the trans beta, trans extended, trans helix, cis beta, cis extended, and cis helix all retained similar dihedral values across all models at the RHF/3-21G and B3LYP/6-31G(d) levels of theory. The topological map (Figure 6, bottom) contains all dihedrals of the structures (**1U** to **6U**) obtained by both optimization levels. The dihedral pairs for the trans isomers were located in eight regions corresponding to the minima in Figure 5 (top). Similarly, extended and beta structures of the cis isomer are also tightly clustered in areas corresponding to the pair of degenerate global minima on the cis-**1U** PES (Figure 5, middle). As shown in supplementary Table 2, the difference between each PUFA chain model with

TABLE 3. Relative Energy, Enthalpy, Free Energy, and Entropy of Models 0U−6U and DHA in kcal mol^{-1}

fragments name		ΔE^0 RHF/3-21G	ΔE^0 B3LYP/ 6-31G(d)	$\Delta E^{0\,a}$ B3LYP/6-311 +G(2d,p)	$\Delta H^{0\,a}$ B3LYP/6-311 +G(2d,p)	$\Delta G^{0\,a}$ B3LYP/6-311 +G(2d,p)	S^b B3LYP/ 6-31G(d)	$\Delta S_{rel}{}^b$ B3LYP/ 6-31G(d)
0U	cis	1.7	1.2	1.3	1.3	1.5	71.910	0.86
	trans	0.0	0.0	0.0	0.0	0.0	71.054	0.00
1U	cis	4.3	3.8	3.6	3.6	3.1	93.738	1.60
		3.6	3.3	3.2	3.2	2.8	93.325	1.18
		3.6	3.3	3.2	3.2	2.8	93.380	1.24
	trans	0.8	0.6	0.7	0.7	0.8	91.582	−0.56
		0.0	0.0	0.0	0.0	0.0	92.038	−0.11
		0.0	0.0	0.0	0.0	0.0	92.143	0.00
2U	cis helix	6.7	6.3	6.0	5.9	5.7	114.449	0.59
	cis extended	5.5	5.1	5.1	5.0	4.5	115.314	1.46
	cis beta	5.6	5.2	5.2	5.0	4.9	114.057	0.20
	trans helix	1.6	1.3	1.6	1.5	2.0	111.912	−1.94
	trans extended	0.0	0.1	0.0	0.0	0.1	113.727	−0.13
	trans beta	0.0	0.0	0.0	0.0	0.0	113.855	0.00
3U	cis helix	9.0	8.8	8.8	8.6	8.4	133.971	0.63
	cis extended	7.5	6.9	6.9	6.7	6.5	134.149	0.81
	cis beta	7.6	6.9	6.9	6.7	6.3	134.870	1.53
	trans helix	2.4	1.8	2.2	2.1	2.3	132.742	−0.60
	trans extended	0.0	0.1	0.1	0.0	0.4	131.948	−1.39
	trans beta	0.0	0.0	0.0	0.0	0.0	133.343	0.00
4U	cis helix	11.2	11.0	11.4	11.1	11.6	153.474	−1.61
	cis extended	9.5	8.7	8.7	8.5	8.0	156.613	1.53
	cis beta	9.6	8.7	8.8	8.5	8.0	156.795	1.71
	trans helix	3.2	2.4	2.9	2.8	3.1	153.895	−1.19
	trans extended	0.0	0.0	0.0	0.0	0.0	154.95	−0.14
	trans beta	0.0	0.0	0.0	0.0	0.0	155.088	0.00
5U	cis helix	13.5	13.3	13.9	13.5	14.7	172.561	−3.86
	cis extended	11.4	10.4	10.5	10.2	9.8	177.909	1.49
	cis beta	11.6	10.6	10.6	10.3	9.8	178.087	1.67
	trans helix	4.0	2.9	3.5	3.4	4.2	173.924	−2.50
	trans extended	0.1	0.0	0.0	−0.1	0.3	175.310	−1.11
	trans beta	0.0	0.0	0.0	0.0	0.0	176.421	0.00
6U	cis helix	15.9	15.4	16.4	16.0	16.9	191.140	−3.14
	cis extended	13.5	11.8	12.2	11.9	9.6	199.147	4.86
	cis beta	13.7	12.3	12.4	12.1	11.0	198.013	3.73
	trans helix	4.9	3.6	4.3	4.1	4.7	192.309	−1.97
	trans extended	0.1	0.0	0.0	−0.1	−0.7	196.353	2.07
	trans beta	0.0	0.0	0.0	0.0	0.0	194.282	0.00

[a] Single point calculation using B3LYP/6-31G(d) geometries. [b] Entropy unit: cal (mol K)$^{-1}$.

the same structure is around ±2°. On the other hand, considerably larger differences were found in all cis helix conformations across all PUFA chain models. However, a closer inspection shows that the behavior of the cis helix in **1U** and **2U** is different from the larger models. The ϕ_1 value of **1U** and **2U** is between 124° and 125°, whereas those in **3U** to **6U** is between 130° and 133°. Furthermore, the second last unit of models **3U** to **6U** seems to have the highest ϕ value. The cis topological map (Figure 6, bottom right) shows that the results, computed at the B3LYP/6-31G(d) level of theory, are more tightly clustered than those at the RHF/3-21G level of theory. Further analysis of the topological map shows that all the cis helix values are distributed in a "dihedral range" corresponding to the smooth basin that is seen in the **1U** surfaces (Figure 5). Therefore, this implies that the large deviation in these dihedral values is the result of many existing minima on the smooth basin of cis PES.

Geometric Properties of Secondary Structures. The side and end view of **5U** are shown in Figure 7 and Figure 8, respectively. These figures show the complete picture of the secondary structures. Here, the names of conformers can be matched with the structural shapes: (A) cis helix is a periodic helical structure of the cis isomer; (B) cis extended is a strand of cis isomer with its double bonds making a series plane rotated 90° with respect to its adjacent double-bond plane; (C) cis beta is a beta strandlike cis isomer with double bonds lined up in planes that rotate in alternating pattern of +90° and −90°; (D) trans helix is a periodic helical structure of the trans isomer; (E) trans extended is a trans isomer that looks like an elongated helix with all trans π-bonds; (F) trans beta looks like a beta strand with all trans π-bonds. The similarity between the helix structures is seen in the hydrogen atoms on the inside and outside of the helices (Figure 8A,D). The inside of the trans helix contains the hydrogens of the sp^2 carbon atoms, and the hydrogen on the inside the cis helix originates from the sp^3 carbon. In both helices, the π-bonds are perpendicular axis of helix. Interestingly, the trans extended resembles a "tube" but has no hydrogen atoms inside (Figure 8E). This heavily influences the relative stability between trans helix and trans extended.

The rotation of the C═C planes can be measured by finding the sum of the corresponding absolute dihedral values $|\phi_i + \psi_i|$. The average values and standard deviations for all plane rotations are listed in Table 4. The averages of the dihedrals are the same for all extended and beta strand models (±2°) and the plane rotation values for the trans helix geometries also remain well established. However, the cis helix has a much larger standard deviation.

The length and other "macro geometrical" properties of the **5U** (belonging to the docosahexanoic acid (DHA) chain) and **6U** structures are summarized in Table 5. The most important feature is the variation of chain length of all the models; the trans beta structure is the longest. The cis extended is 2.5 times

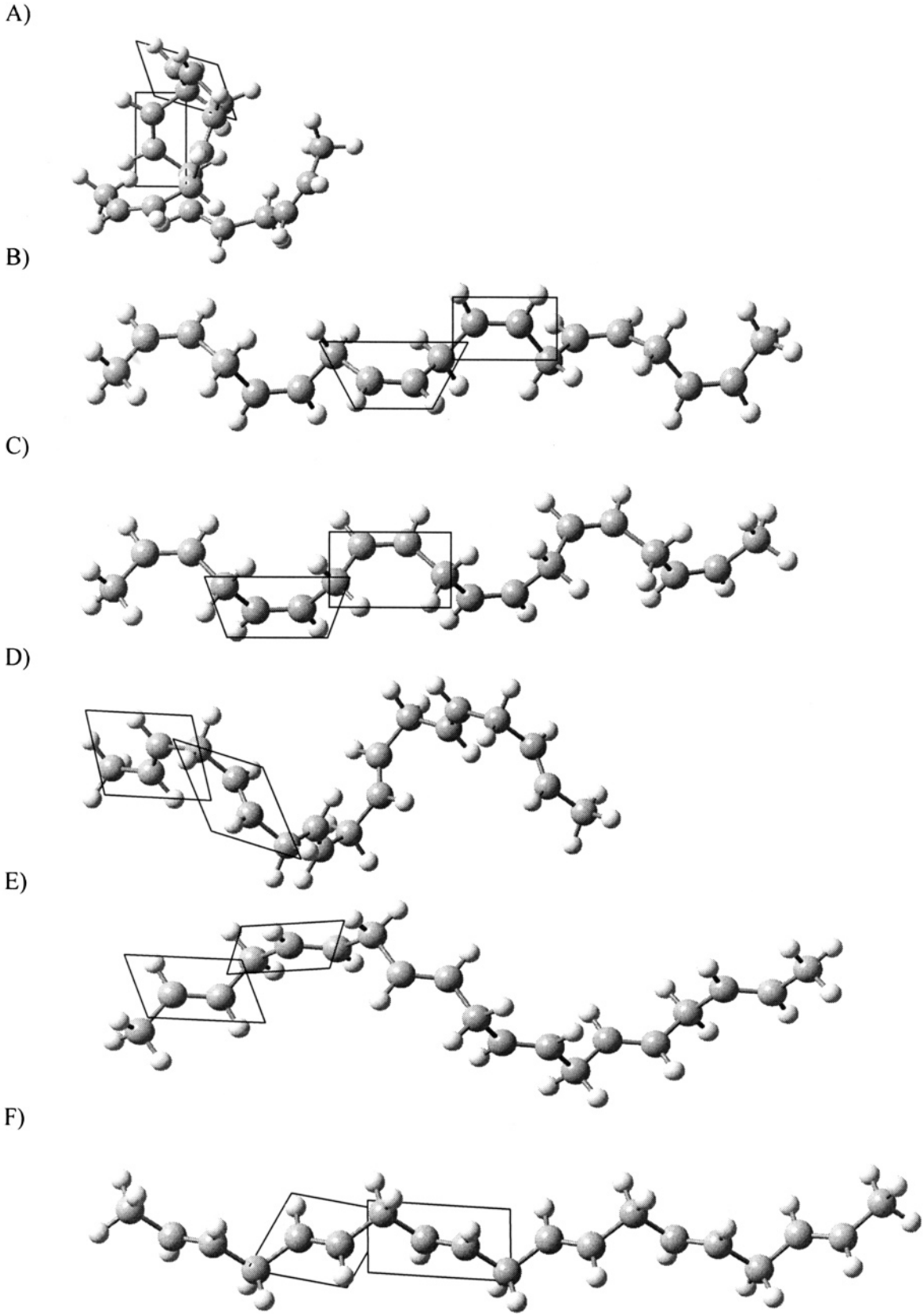

Figure 7. Side view of the DHA chain (**5U** model) optimized by B3LYP/6-31G(d) level of theory. A−F are the cis helix, cis extended, cis beta, trans helix, trans extended, and trans beta structure, respectively.

longer than the helix structure. Also, smaller differences were found among the trans isomers. The diameter of the helix can be calculated using the formula

$$d = \sqrt{c^2 - b^2} \tag{3}$$

It should be noted that the points C_2 and C_{15} and the midpoint between C_2 and C_{29} forms a right angle triangle. Therefore, c is the distance between C_2 and C_{15} and b is half the distance between C_2 and C_{29}. Having measured these two distances, the diameter d can be calculated using eq 3.

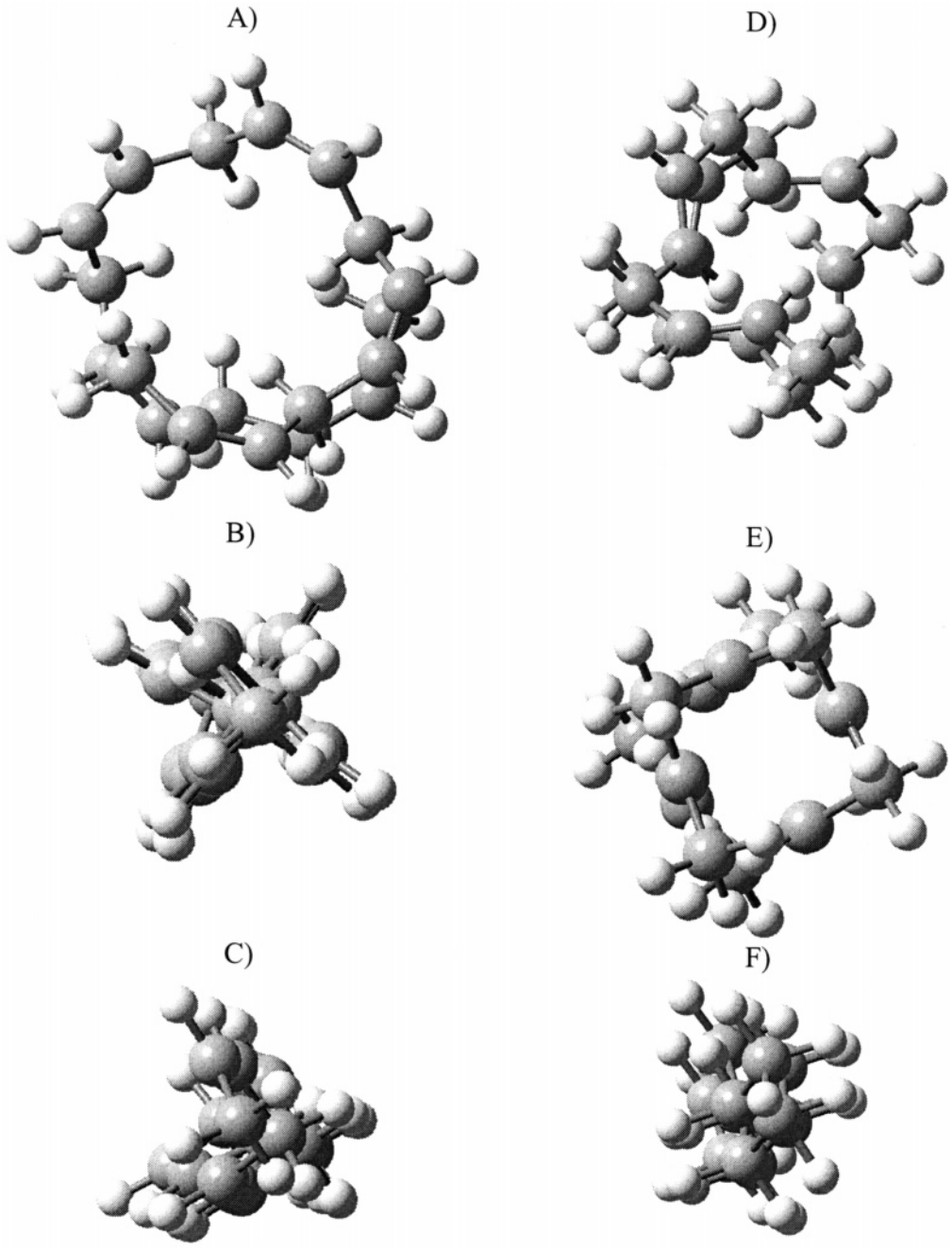

Figure 8. Top view of the DHA chain (**5U** model). A−F are the cis helix, cis extended, cis beta, trans helix, trans extended, and trans beta structure, respectively.

TABLE 4. Distribution of the Angles (θ) of the Adjacent C═C Bond Planes for the Six Conformational Groups

conformational group	θ/deg (average)
cis helix	75.5 ± 7.7
cis extended	53.2 ± 1.4
cis beta	55.2 ± 2.2
trans helix	48.8 ± 0.8
trans extended	55.8 ± 0.8
trans beta	56.2 ± 1.7

The diameters of the helices at 4.7 Å may allow for opening of hydrophobic "channels" within the membranes. The inside diameter of the "tube" of cis helix is about 3.5 Å, which takes into account the interior H atoms. Thus, the membrane with unsaturated fatty acids can become permeable for small molecules (i.e., N═O, CO_2, H_2O). The other important point is the variation in chain length by a factor of 2. Such a change can cause the membrane thickness to vary. The latter property was also suggested by earlier MM calculation,[10] but the energy needed for such motions could not be calculated.

Table 6 shows selected sigma bond length of the helical structures. It is interesting to note that the chiralty of helicity affected the geometry of the CH_2 groups. In the case of the trans isomers, the C−C bond length differed by almost 0.01 Å, and the pair of C−H bonds also differed by 0.002 Å. The change in C−C bond length was dominant. In contrast, the C−H bond length in the cis isomer was dominant, differing by 0.01 Å, while the C−C bond length changing was negligible at 0.003 Å.

Thermochemistry of Secondary Structures. The relative energies (ΔE_{rel}) corrected by scaled ZPE of the conformations are listed in Table 3. The reference structure with the most stable conformer, the trans beta, was chosen, with $\phi_i = \psi_i \sim 120°$

TABLE 5. Geometrical Parameters of Secondary Structures for 5U and 6U Optimized at B3LYP/6-31G(d) Level of Theory (Length in Å)

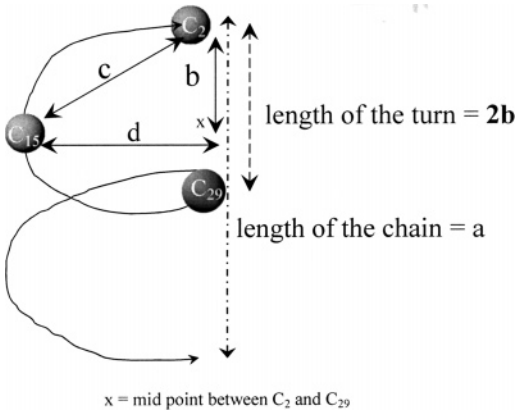

	structure	*a* C_2 to C_n	2*b* C_2 to C_{29}	*c* C_2 to C_{15}	*d* diameter
5U	cis helix	7.4	4.1	5.1	4.7
	cis extended	19.1			
	cis beta	19.0			
	trans helix	14.4	9.1	6.4	4.4
	trans extended	18.6			
	trans beta	21.3			
6U	cis helix	8.7	4.2	5.1	4.6
	cis extended	22.4			
	cis beta	22.1			
	trans helix	16.1	9.0	6.4	4.5
	trans extended	21.8			
	trans beta	24.4			

and $\phi_{i+1} = \psi_{i+1} \sim -120°$ dihedrals. The cis−trans isomerization enthalpy ΔH_{isom} for the hydrocarbon chains was obtained by calculating the enthalpy between the cis and trans isomers of the same conformers:

$$\Delta H_{isom} = \Delta H_{cis} - \Delta H_{trans} \quad (4)$$

where ΔH_{cis} and ΔH_{trans} are the relative enthalpies of corresponding conformers of all units (**0U**−**6U**).

Same conformations of the cis and trans isomers were paired for each model, and as expected, all trans conformers are more stable than their cis counterpart. Comparison of the enthalpy of cis **0U** and trans **0U** shows that there is a difference of about 1.5 kcal mol^{-1} between the cis and trans isomers with one double bond. This finding is in good agreement with the experimental enthalpy of formation difference of *cis*- and *trans*-2-butene[35] of 1.1 kcal mol^{-1}. The relationship between the relative energy of cis−trans isomers of the allylic molecules and the degree of polymerization was also investigated according to Benson's group additivity rules.[36] As suggested earlier, the additivity rules are excellent and sensitive tools to estimate the change in accuracy with size.[37] Figure 9 suggests that there is a strong correlation between the number of units and the cis−trans isomerization enthalpy for all models. The relative isomerization enthalpy for all cis−trans pair is 1.7 ± 0.2 kcal mol^{-1} unit^{-1}. It is expected that this relative isomerization energy trend can be applied to all cis−trans conformer pairs of such nondirect, i.e., hyperconjugative delocalized π-electron systems. The strong correlation between the relative enthalpy and degree of polymerization can also confirm our selection strategy of conformers.

The enthalpy difference between the helix and the extended conformers could be defined as the folding enthalpy differences between an extended chain and a folded complex structure of the trans as well as cis helix.

$$\Delta H_{folding} = \Delta H_{helix} - \Delta H_{beta} \quad (5)$$

As can be seen in Figure 10, the destabilization effect also increases with the folding. We have to take in account that such fine effects in energy are measurable within the expected error of the theoretical model used. This increase in enthalpy of folding is smaller than expected on the basis of steric repulsion. Presumably it is due to concurrent van der Waals stabilization; no $\pi\cdots$H−C hydrogen bond is present in the helical conformation. The increase in folding energy from all helix-extended pairs, $\Delta H_{folding}$, is 0.5 ± 0.1 kcal mol^{-1} unit^{-1}. This relative conformational energy trend may be able to predict helix-extended conformer pairs of such nondelocalized π-electron systems. For DHA (**5U**), the change in the length of the cis structure by a factor of 2 may require less than 2.5 kcal mol^{-1} in enthalpy. This small conformational enthalpy value may be allowed for polyunsaturated fatty acids to determine macroscopic membrane properties. The **6U** folding energy in the cis isomer is 0.4 kcal mol^{-1} lower than expected. This is due to systematic error in procedure of optimization that is very likely to occur in the cis helix because this structure produces a very flat PES on which many minima are possible in a given area of the surface.

The data presented in Table 3 reveals that the entropy change associated with folding

$$\Delta S_{folding} = S_{helix} - S_{beta}$$

decreases faster with size (*n*) for the cis isomer than for the trans isomer as shown graphically in Figure 11. Clearly, the cis helix is more compact (Figure 7A) than the trans helix (Figure 7D). Such difference in trend of entropy change, as shown in Figure 11, is the basis for the variation of Gibbs free energy change of folding with *n* (Figure 12)

$$\Delta G_{folding} = \Delta G_{helix} - \Delta G_{beta}$$

It can be concluded at the end of our study that the large flexibility observed is a result of two structure characteristic unique to allylic systems: (i) the cis double bond in the 1,4-position and (ii) the CH_2 groups with two quasi-free rotor in 2,4-positions. This is in excellent agreement with the solid-state NMR measurements.[18] They have predicted that DHA is an extreme flexible molecule with rapid transitions between large numbers of conformers on the time scale from picoseconds to hundreds of nanoseconds.[18]

Comparisons Allylic Chains and Peptide Backbones. The structures of allylic fragments are very similar to those of the peptide backbone, especially to polyglycyl peptides, which has an isoelectronic skeleton backbone. Therefore, the modular pattern seen in peptide models can also be found in allylic chains. In turn, this means that structures between these two classes of molecules are comparable. In this section, the similarities as well as the differences found between the allylic system and the polypeptides[38] will be discussed.

Ab initio computations have shown that a single glycine residue is unable to form stable left-handed ($\phi \approx \psi \approx 60°$) and right-handed ($\phi \approx \psi \approx -60°$) α-helix;[39] however, it is able to form β-strands[39] with $\phi \approx \psi \approx 180°$. Furthermore, the δ_L ($\phi \approx -126.0°$, $\psi \approx 25.5°$) helix also exists in the peptide model.[39] Such δ_L structures are found at the end of many peptide helices as a $\alpha_L\delta_L$ motif, which are suggested to be a termination of certain helices.[40] Other existing peptide structures[39] such as $\gamma_{D/L}$

TABLE 6. Geometrical Diagnostics of Helicity-Induced Point Chirality of CH_2 Groups in Helical Conformers of 5U (Bond Lengths in Å)

	trans helix				cis helix			
	C_n-C_{n-1}	C_n-C_{n+1}	C_n-H_{n+3}	C_n-H_{n+4}	C_n-C_{n-1}	C_n-C_{n+1}	C_n-H_{n+3}	C_n-H_{n+4}
C_8	1.505	1.514	1.101	1.103	1.512	1.511	1.093	1.103
C_{15}	1.505	1.514	1.101	1.103	1.514	1.511	1.094	1.103
C_{22}	1.505	1.514	1.101	1.103	1.514	1.512	1.094	1.103
C_{29}	1.505	1.514	1.101	1.103	1.515	1.511	1.093	1.103
C_{36}	1.505	1.514	1.101	1.103	1.514	1.512	1.093	1.103

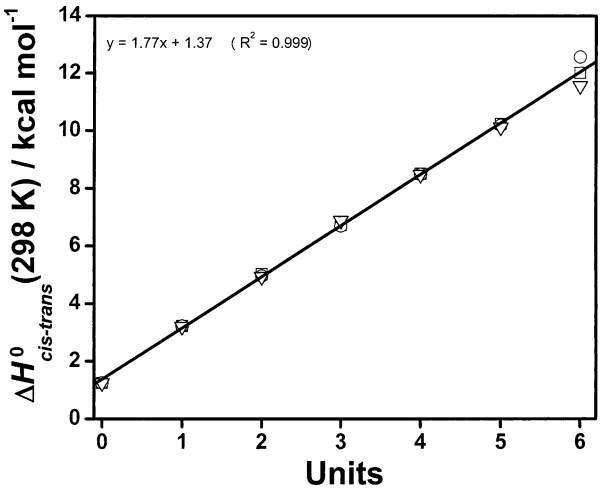

Figure 9. Relative enthalpy of cis/trans isomerization of extended (○), beta (□), and helix (▽) conformation pairs as a function of the number of units.

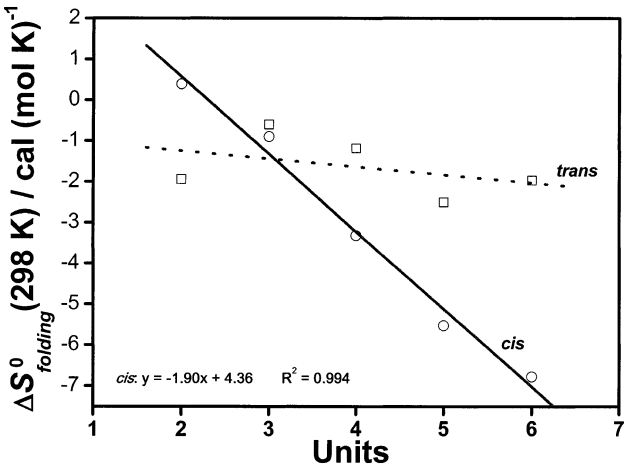

Figure 11. Relative entropy of folding as a function of the number of units: □ represents the folding entropy of all trans isomers of **1U** to **6U**, and ○ represents the folding entropy of all cis isomers of **2U** to **6U**.

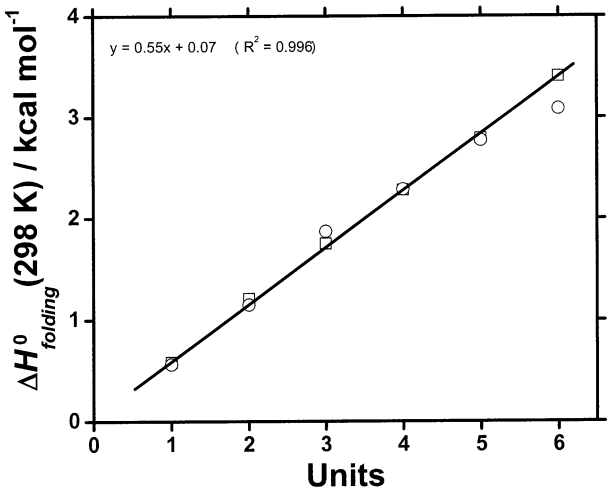

Figure 10. Relative enthalpy of folding as a function of the number of units: □ represents the folding energy of all trans isomers of **1U** to **6U**, and ○ represents the folding energy of all cis isomers of **2U** to **6U**.

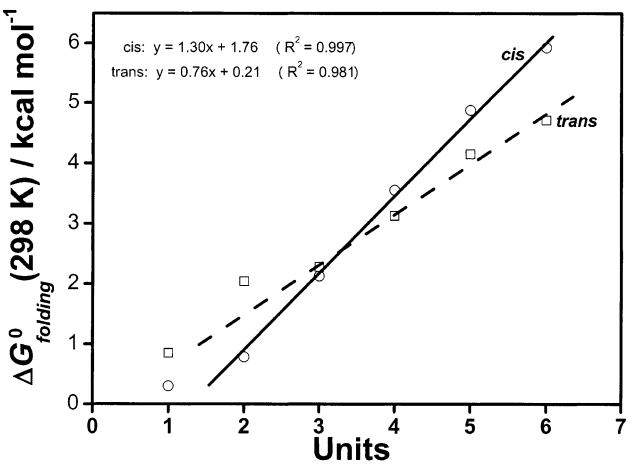

Figure 12. Gibbs free energy of folding as a function of the number of units: □ represents the folding energy of all trans isomers of **1U** to **6U**, and ○ represents the folding energy of all cis isomers of **2U** to **6U**.

are unimportant in the case of PUFA chains and therefore not investigated in the present work. Comparisons between the peptide model and the PUFA model cis helix seem to indicate that the two molecules have a similar macrostructures. The key to similarity resides in molecular flexibility. Thus, one may wonder whether flexibility predestinated these macromolecules to fulfill multitudes of biological function.

Upon closer inspection, the cis helix contains all cis double bonds, whereas the peptide helix usually contains trans double bonds. Furthermore, comparison between the dimensions of the two models shows that in the peptide helix is around 5 Å, and it is somewhat similar to the cis helix that has a diameter around 4.7 Å. The pitch of the peptide α-helix that has hydrogen bonds is about 5.4 Å, which is a lot longer than the cis helix that is only between 4.1 and 4.2 Å and has no hydrogen bonds. Although similar in macrostructure, the peptide helix and the cis helix differ in their microstructure. The similarity between a cis PUFA helix and a peptide helix suggests that trans membrane proteins do not disturb considerably more the structure of lipid bilayer than the inclusion of PUFA in the component phospholipids.

On the other hand, comparisons between the polypeptide α-helix and trans helix reveal that both helices are trans isomers. Therefore, both of these models can be compared to a peptide helix. The trans helix model also contains hydrogens positioned inside the coil, and such observation is not found in peptides. Furthermore, the diameter of the trans helix is also smaller than

that of a peptide α-helix. Therefore, the cis helix is geometrically considerably similar to the α-helix than that of the trans helix. Generally, the flexibility of peptide backbones is similar to the cis helix, but for special positions where the free rotation is sterically allowed for allylic fragments, the peptide will not be able to rotate freely as a result of intramolecular H bonds. It is interesting to note that through molecular evolution biological systems prefer to use such flexible building blocks such as peptides and cis unsaturated fatty acids to synthesize the macromolecular system.

Conclusions

The Hartree−Fock and density functional theory methods were used to study the high flexibility of the PUFA chain fragments. The fragments allowed us to study, in small consecutive steps, the folding effects of the chain as the function of fragment length. The topology of the energy minima distribution on the PES of the smallest model of cis **2U** showed the existence of a special "smooth basin" in the area where the cis helix is located. Because of the flat nature of this the basin, many minima could be found. This is consistent with the large deviation in dihedral values found in the cis helix of different models.

In principle, the chain of **5U** has $2^6 \times 3^{14}$ conformational minima. Here we have investigated a few conformers with geometries similar to helices and straight chains. These geometries were constructed by repeating a specific dihedral pattern found in the cis **2U** model. For this study, the length of the cis DHA helices and straight chains varied between 9.8 and 22 Å, respectively. However, such marked geometric differences correspond only to a change of about 2.5 kcal mol^{-1} in enthalpy. Also, there is striking conformational similarity between the trans helix of 1,4-polyenes and the δ-helix of polyglycine. The folding energy of 0.5 kcal mol^{-1} unit^{-1} has be extracted from the energy comparison of the helixes and most extended structures. We addressed the question of whether the folding energy obtained in the present study could be applied in more general use to describe the thermochemistry of protein folding with particular reference to membrane proteins as they are exposed to the same environment as cis PUFA molecules such as cis DHA.

Acknowledgment. The authors thank M. Labadi for technical support, Michelle A. Sahai for helpful discussions, and Odon Farkas for the construction of the *N*-Ac-Gly-NHMe PES. I.G.C. thanks the Ministry of Education for a Szent-Györgyi Visiting Professorship. The authors are grateful to the Hungarian Scientific Research Fund (OTKA T046861 and F037648).

Supporting Information Available: Table of relative energies and dihedral values of **2U** and dihedrals of **0U**−**6U**. This material is available free of charge via the Internet at http://pubs.acs.org.

References and Notes

(1) Acar, N.; Chardigny, J.; Bonhomme, B.; Almanza, S.; Doly, M.; Sébédio, J. *J. Nutr.* **2002**, *132*, 3151−3154.

(2) Feller, S. E.; Gawrisch, K.; MacKerell, A. D. *J. Am. Chem. Soc.* **2002**, *124*, 318−326.

(3) Stryer, R. *Biochemistry* ; W.H. Freeman and Co.: New York, 1995; pp 27−32.

(4) Olbrich, K.; Rawicz, W.; Needham, D.; Evans, E. *Biophys. J.* **2000**, *79*, 321−327.

(5) Niebylski, C. D.; Salem, N., Jr. *Biophys. J.* **1994**, *67*, 2387−2393.

(6) Mitchell, D. C.; Litman, B. J. *Biophys. J.* **1998**, *74*, 879−891.

(7) Alexander-North, L. S.; North, J. A.; Kiminyo, K. P.; Buettner, G. R.; Spector, A. A. *J. Lipid Res.* **1994**, *35*, 1773−1785.

(8) Murphy, R. C. *Chem. Res. Toxicol.* **2001**, *14*, 463−472.

(9) Markesbery, W. R. *Free Radical Biol. Med.* **1997** *23*, 134−147.

(10) Applegate, K. R.; Glomset, J. A. *J. Lipid Res.* **1986**, *27*, 658−680.

(11) Rich, M. R. *Biochem. Biophys. Acta* **1993**, *1178*, 87−96.

(12) Shimanouchi, T.; Abe, Y.; Alaki, Y. *Bull. Chem. Soc. Jpn.* **1971**, *48*, 3557−3560.

(13) Schurinck, W. T.; de Jong, S. *Chem. Phys. Lipids* **1977**, *19*, 313−322.

(14) Albrand, M.; Pageaux, J.; Lagarde, M.; Dolmazon, R. *Chem. Phys. Lipids* **1994**, *72*, 7−17.

(15) van Hemelrijk, D.; van den Enden, L.; Geise, H. J. *J. Mol. Struct.* **1981**, *74*, 123−135.

(16) Albrand, M.; Pageaux, J.; Lagarde, M.; Dolmazon, R. *Chem. Phys. Lipids* **1994**, *72*, 7−17.

(17) Bachar, M.; Brunelle, P.; Tieleman, D. P.; Rauk, A. *J. Phys. Chem. B* **2004**, *108*, 7170−7179.

(18) Gawrisch, K.; Eldho, N. V.; Holte, L. L. *Lipids* **2003**, *38*, 445−452.

(19) Baenziger, J. E.; Jarrell, H. C.; Hill, H. C.; Smith, I. C. P. *Biochemistry* **1991**, *30*, 894−903.

(20) Balendiran, G. K.; Schnutgen, F.; Scapin, G.; Borchers, T.; Xhong, N.; Lim, K.; Godbout, R.; Spener, F.; Sacchettini, J. C. *J. Biol. Chem.* **2000**, *275*, 27045−27054.

(21) Egea, P. F.; Mitschler, A.; Moras, D. *Mol. Endocrinol.* **2002**, *16*, 987−997.

(22) Voet, D.; Voet, J. G. *Biochemistry*, 1st ed.; John Wiley & Sons: New York, 1990; pp 149−152.

(23) Dinner, A. R.; Lazaridis, T.; Karplus, M. *Proc. Natl. Acad. Sci. U.S.A.* **1999**, *96*, 9068−9073.

(24) Worth, G. A.; Wade, R. C. *J. Phys. Chem.* **1995**, *99*, 17473−17482.

(25) Nardi, F.; Kemmink, J.; Sattler, M.; Wade, R. C. *J. Biomol. NMR* **2000**, *17*, 63−77.

(26) Borics, A.; Chass, G. A.; Csizmadia, I. G.; Murphy, R. F.; Lovas, S. *J. Mol. Struct. (THEOCHEM)* **2003**, *666*−*667*, 355−359.

(27) Sheraly, A. R.; Chang, R. V.; Chass, G. A. *J. Mol. Struct. (THEOCHEM)* **2002**, *619*, 21−35.

(28) Liao, J. C. C.; Chua, J. C.; Chass, G. A.; Perczel, A.; Varro, A.; Papp, J. Gy. *J. Mol. Struct. (THEOCHEM)* **2003**, *621*, 163−187.

(29) Chass, G. A.; Sahai, M. A.; Law, J. M. S.; Lovas, S.; Farkas, Ö.; Perczel, A.; Csizmadia, I. G. *Int. J. Quantum Chem.* **2002**, *90*, 933−968.

(30) Sahai, M. A.; Lovas, S.; Chass, G. A.; Penke, B.; Csizmadia, I. G. *J. Mol. Struct. (THEOCHEM)* **2003**, *666*−*667*, 169−218.

(31) Scott, A. P.; Radom, L. *J. Phys. Chem.* **1996**, *100*, 16502−16513.

(32) Frisch, M. J.; Trucks, G. W.; Schlegel, H. B.; Scuseria, G. E.; Robb, M. A.; Cheeseman, J. R.; Zakrzewski, V. G.; Montgomery, J. A., Jr.; Stratmann, R. E.; Burant, J. C.; Dapprich, S.; Millam, J. M.; Daniels, A. D.; Kudin, K. N.; Strain, M. C.; Farkas, O.; Tomasi, J.; Barone, V.; Cossi, M.; Cammi, R.; Mennucci, B.; Pomelli, C.; Adamo, C.; Clifford, S.; Ochterski, J.; Petersson, G. A.; Ayala, P. Y.; Cui, Q.; Morokuma, K.; Malick, D. K.; Rabuck, A. D.; Raghavachari, K.; Foresman, J. B.; Cioslowski, J.; Ortiz, J. V.; Stefanov, B. B.; Liu, G.; Liashenko, A.; Piskorz, P.; Komaromi, I.; Gomperts, R.; Martin, R. L.; Fox, D. J.; Keith, T.; Al-Laham, M. A.; Peng, C. Y.; Nanayakkara, A.; Gonzalez, C.; Challacombe, M.; Gill, P. M. W.; Johnson, B. G.; Chen, W.; Wong, M. W.; Andres, J. L.; Head-Gordon, M.; Replogle, E. S.; Pople, J. A. *Gaussian 98*, revision, A.7; Gaussian, Inc.: Pittsburgh, PA, 1998.

(33) Frisch, M. J.; Trucks, G. W.; Schlegel, H. B.; Scuseria, G. E.; Robb, M. A.; Cheeseman, J. R.; Montgomery, J. A., Jr.; Vreven, T.; Kudin, K. N.; Burant, J. C.; Millam, J. M.; Iyengar, S. S.; Tomasi, J.; Barone, V.; Mennucci, B.; Cossi, M.; Scalmani, G.; Rega, N.; Petersson, G. A.; Nakatsuji, H.; Hada, M.; Ehara, M.; Toyota, K.; Fukuda, R.; Hasegawa, J.; Ishida, M.; Nakajima, T.; Honda, Y.; Kitao, O.; Nakai, H.; Klene, M.; Li, X.; Knox, J. E.; Hratchian, H. P.; Cross, J. B.; Adamo, C.; Jaramillo, J.; Gomperts, R.; Stratmann, R. E.; Yazyev, O.; Austin, A. J.; Cammi, R.; Pomelli, C.; Ochterski, J. W.; Ayala, P. Y.; Morokuma, K.; Voth, G. A.; Salvador, P.; Dannenberg, J. J.; Zakrzewski, V. G.; Dapprich, S.; Daniels, A. D.; Strain, M. C.; Farkas, O.; Malick, D. K.; Rabuck, A. D.; Raghavachari, K.; Foresman, J. B.; Ortiz, J. V.; Cui, Q.; Baboul, A. G.; Clifford, S.; Cioslowski, J.; Stefanov, B. B.; Liu, G.; Liashenko, A.; Piskorz, P.; Komaromi, I.; Martin, R. L.; Fox, D. J.; Keith, T.; Al-Laham, M. A.; Peng, C. Y.; Nanayakkara, A.; Challacombe, M.; Gill, P. M. W.; Johnson, B.; Chen, W.; Wong, M. W.; Gonzalez, C.; Pople, J. A. *Gaussian 03*, revision B.01; Gaussian, Inc.: Pittsburgh, PA, 2003.

(34) Law, J. M. S.; Szori, M.; Csizmadia, I. G.; Viskolcz, B., to be published.

(35) Holden, N. E. *CRC Handbook: Handbook of Chemistry and Physics*, 84h ed.; CRC Press Inc.: Boca Raton, FL, 2003.

(36) Benson, S. W. *Thermochemical Kinetics*; John Wiley and Sons: New York, 1976.

(37) Marsi, I.; Viskolcz, B.; Seres, L. *J. Phys. Chem. A* **2000**, *104*, 4497−4504.

(38) Chass, G. A. *J. Mol. Struct. (THEOCHEM)* **2003**, *666*−*667*, 61−67.

(39) Mehdizadeh, A.; Chass, G. A.; Farkas, O.; Perczel, A.; Torday, L. L.; Varro, Papp, J. Gy. *J. Mol. Struct.* (*THEOCHEM*) **2002**, *588*, 187−200.

(40) Perczel, A.; Endredi, G.; McAllister, M. A.; Farkas, O.; Csaszar, P.; Csizmadia, I. G. *J. Mol. Struct. (THEOCHEM)* **1995**, *331*, 5−10.

(41) Topol, I. A.; Burt, S. K.; Deretey, E.; Tang, T.-H.; Perczel, A.; Rashin, A.; Csizmadia, I. G. *J. Am. Chem. Soc.* **2001**, *123*, 6054−6060.